Integrated Cooperative Control Scheme for Multiple Quadrotors Based on Improved Adaptive Disturbance Rejection Control

Han Du, Zhiqiang Pu, Jianqiang Yi

Abstract— **This paper presents an integrated cooperative control scheme for multiple quadrotors. The design of cooperative control scheme mainly consists of the upper formation controller and the bottom trajectory tracking controller. Firstly the "leader-follower" formation model and the quadrotor dynamic model are established, with trajectory tacking errors, measurement errors and communication time delay concerned. On one hand, the extended state observer (ESO) is constructed to estimate and attenuate the disturbances for the formation controller. The communication time delay is handled with the specially designed improved adaptive disturbance rejection control (ADRC) law. On the other hand, the trajectory tracking controller is realized using double-loop control laws, which are the dynamic inversion (DI) law in the outer loop and back-stepping law in the inner loop. The stability of the closed-loop system is analyzed with the Lyapunov method. Finally, a series of simulations are conducted to validate the effectiveness of integrated cooperative control scheme.**

I. INTRODUCTION

Featuring variable formations and flexible cooperating ways, multiple quadrotors have advantages over single one in complex mission accomplishment. The main investigations in the formation control are composed as follows: the assignment of feasible formations [1], the smooth process of formation establishment [2], the maintenance of formation shape [3], and the transitions to other formations [4]. There are three different main approaches proposed to solve the challenges above, which are utilized strategies based on the leader-follower model [4, 5], the virtual structure [6], and the weighted behavior mechanism [7] respectively. The leader-follower model is useful in practical realization, in which the lead quadrotor tracks the desired trajectory given by ground station, and the follower tracks the trajectory generated by the desired formation and motion of the lead quadrotor.

The cooperative control of the multiple quadrotors consists of the upper formation control and the bottom trajectory tacking control. The formation control provides reference trajectory for the bottom control. For reference trajectories generated by the formation control need to be tracked rapidly and precisely, the trajectory tracking control should be effective and robust enough. Conversely, the tracking errors are unavoidable in the bottom trajectory tracking control, which lead to the disturbances in the formation control. There hasn't been a satisfying integrated cooperative control scheme for the challenge above. In [8], the agent trailing control was cast into a stability problem. By improving the input-to-state stability (ISS) method, the control realized robustness against small measurement noises and disturbances. Lozano [9] considered both coordination and trajectory controls of multiple quadrotors with state feedback controllers. However, the disturbances in coordination control were not taken into account. Active disturbance rejection control (ADRC) [10] provides a better key to disturbance rejection in the formation control. The centerpiece of ADRC is taking all internal uncertainties and external disturbances considered together, treating it as an extended state to be directly estimated with extended state observer (ESO).The communication delay is another unneglectable challenge in the cooperative control. Gao [11] proposed a modified ADRC control law to handle the system with transport delay by control prediction. For the quadrotor trajectory tracking control, many nonlinear controllers have been designed, just as back-stepping [12], sliding mode [13], and incremental dynamic inversion [14]. The ADRC can be combined with those existed controllers to improve the robustness in trajectory tracking control.

In this paper a integrated cooperative control scheme is proposed for multiple quadrotors. Firstly, the formation dynamic model is established, with the tracking errors, measurement errors and time delays taken into account. Secondly, ESO is incorporated in the formation controller design to reject disturbances and make the formation switch smooth. Thirdly, the specially designed improved ADRC is constructed to cope with the communication delay in the formation control. Finally, the robustness is concerned adequately in the integrated cooperative control scheme.

II. DYNAMIC MODELS

A. Leader-Follower Formation Dynamic Model

The states of quadrotor in the formation is described by the $S_i=(\mathbf{X}_i,\mathbf{V}_i,\boldsymbol{\xi}_i,\boldsymbol{\Omega}_i)$. $\mathbf{X_i}=(x_i,y_i,z_i)^T$ and $\mathbf{V_i}=(u_i,v_i,w_i)^T$ denote the position and speed in the earth frame. $\boldsymbol{\xi_i}=(\phi_i,\theta_i,\psi_i)^T$ and $\boldsymbol{\Omega_i}=(p_i,q_i,r_i)^T$ are the angles and angular rates. The one-leader-one-follower dynamic model is described by the lead quadrotor (S_1) and the follow quadrotor (S_2), which can be expanded to the one-leader-multi-followers formation model.

*Resrach supported by Foundation under grant #61273149, #61421004, #B1320133020, and #CXJJ-16Z212.

Han Du is with University of Chinese Academy of Sciences and Institute of Automation, Chinese Academy of Sciences, Beijing, 100190 China, (e-mail: duhan2014@ia.ac.cn).

Zhiqiang Pu is with Institute of Automation, Chinese Academy of Sciences, Beijing, 100190 China, (corresponding author to provide phone: 86-010-82544639; e-mail: zhiqiang.pu@ia.ac.cn)

Jianqiang Yi is with Institute of Automation, Chinese Academy of Sciences, Beijing, 100190 China, (e-mail: jianqiang.yi@ia.ac.cn).

To establish the one-leader-one-follower model, the relative motion frame $M=(x_m,y_m,z_m)^T$ is established by rotating the yaw angle of the leader ψ_1 around the z axis of the earth frame $E=(x,y,z)^T$. The coordinates in the two frames satisfy

$$\begin{bmatrix} x_{mi} \\ y_{mi} \\ z_{mi} \end{bmatrix} = \begin{bmatrix} \cos\psi_1 & \sin\psi_1 & 0 \\ -\sin\psi_1 & \cos\psi_1 & 0 \\ 0 & 0 & 1 \end{bmatrix} \begin{bmatrix} x_i \\ y_i \\ z_i \end{bmatrix} \tag{1}$$

Denoting the relative distances as $\lambda_x, \lambda_y, \lambda_z$, the relative yaw angle as λ_ψ, where

$$\begin{cases} \lambda_x = x_{m2} - x_{m1} = (x_2 - x_1)\cos\psi_1 + (y_2 - y_1)\sin\psi_1 \\ \lambda_y = y_{m2} - y_{m1} = (y_2 - y_1)\cos\psi_1 - (x_2 - x_1)\sin\psi_1 \\ \lambda_z = z_{m2} - z_{m1} = z_2 - z_1 \\ \lambda_\psi = \psi_2 - \psi_1 \end{cases} \tag{2}$$

The derivate equations of (2) are given as

$$\begin{cases} \dot{\lambda}_x = \lambda_y r_1 + \cos\psi_1(u_2 - u_1) + \sin\psi_1(v_2 - v_1) \\ \dot{\lambda}_y = -\lambda_x r_1 + \cos\psi_1(v_2 - v_1) - \sin\psi_1(u_2 - u_1) \\ \dot{\lambda}_z = w_2 - w_1 \\ \dot{\lambda}_\psi = r_2 - r_1 \end{cases} \tag{3}$$

which serves as the one-leader-one-follower formation model. For the multiple quadrotor system can be regarded as the combination of many leader-follower pairs, the formation model of one-leader-multi-followers is expanded from (3).

B. Quadrotor Dynamic Model

The multiple quadrotors share the same dynamic model, which is formulated according to the Newton-Euler function

$$\left.\begin{aligned} \sum F &= \mathbf{1}_v \frac{\delta \mathbf{V}}{\delta t} + \boldsymbol{\Omega} \times \mathbf{V} \\ \sum M &= J\dot{\boldsymbol{\Omega}} + \boldsymbol{\Omega} \times J\boldsymbol{\Omega} \end{aligned}\right\|, J = \begin{bmatrix} I_x & 0 & 0 \\ 0 & I_y & 0 \\ 0 & 0 & I_z \end{bmatrix} \tag{4}$$

where J is the inertia matrix, $\sum F$ and $\sum M$ are the resultant forces and resultant moments of the quadrotor. Based on (4), the quadrotor dynamic model can be briefly given as

$$\begin{aligned} &\dot{\mathbf{X}}=\mathbf{V} \quad \dot{\boldsymbol{\xi}}=\boldsymbol{\Omega} \\ &\ddot{x} = (\sin\psi\sin\phi + \cos\psi\sin\theta\cos\phi)\frac{F}{m} + \Delta f_x \\ &\ddot{y} = (-\cos\psi\sin\phi + \sin\psi\sin\theta\cos\phi)\frac{F}{m} + \Delta f_y \\ &\ddot{z} = (\cos\theta\cos\phi)\frac{F}{m} - g + \Delta f_z \\ &\ddot{\phi} = \frac{I_y - I_z}{I_x} qr + \frac{1}{I_x}\tau_\phi + \Delta f_\phi \\ &\ddot{\theta} = \frac{I_z - I_x}{I_y} pr + \frac{1}{I_y}\tau_\theta + \Delta f_\theta \\ &\ddot{\psi} = \frac{I_x - I_y}{I_z} pq + \frac{1}{I_z}\tau_\psi + \Delta f_\psi \end{aligned} \tag{5}$$

where $\Delta f_x, \Delta f_y, \Delta f_z, \Delta f_\phi, \Delta f_\theta, \Delta f_\psi$ are disturbances and unmodeled dynamics. F is the total thrust force and $\tau_\phi, \tau_\theta, \tau_\psi$ are the torques in three directions. Denoting $w_1 \sim w_4$ as the speed of four rotors, k_T and k_d as the lift and the propeller torque coefficients respectively, l as the distance between each rotor and the gravity center of the quadrotor, there is

$$\begin{bmatrix} F \\ \tau_\phi \\ \tau_\theta \\ \tau_\psi \end{bmatrix} = \begin{bmatrix} lk_T & lk_T & lk_T & lk_T \\ 0 & -lk_T & 0 & lk_T \\ lk_T & 0 & -lk_T & 0 \\ k_d & -k_d & k_d & -k_d \end{bmatrix} \begin{bmatrix} w_1^2 \\ w_2^2 \\ w_3^2 \\ w_4^2 \end{bmatrix} \tag{6}$$

III. Design of The Formation Controller

A. Design of the Formation Controller

The entire integrated cooperative control scheme is depicted in Figure 1. The one-leader-one-follower scheme can be applied to all the leader-follower pairs, thus realizing the one-leader-multi-quadrotors formation control. The formation controller is located in the ground station, which has access to all measurable states of the multiple quadrotors, and is responsible for the the assignment of the lead quadrotor's reference trajectory. For the ground station, the states of the lead quadrotor are available and can be utilized to generate reference trajectories for the followers. The security of the ground station is guaranteed. When the lead quadrotor gets in trouble, one of the followers would be selected as the "new leader" by the ground station, and the rest quadrotors reestablish the new formation

The tracking errors in the trajectory control and the measurement errors of the multiple quadrotor states are unavoidable, which are taken together and formulated as $\boldsymbol{\Delta}(t)$. What's worse, there inevitably exists radio communication delay in the formation system, which is formulated as τ. The value of τ depends on the type of radio and can be estimated by experiments. Denoting $\boldsymbol{\lambda}=(\lambda_x,\lambda_y,\lambda_z,\lambda_\psi)^T$, the nonlinear time-delay formation system can be formulated as

$$\begin{aligned} &\dot{\boldsymbol{\lambda}}(t) = f(\boldsymbol{\lambda}) + \mathbf{u}(t-\tau) + \boldsymbol{\Delta}(t) \\ &f(\boldsymbol{\lambda}) = \begin{bmatrix} \lambda_y r_1 - \cos\psi_1 u_1 - \sin\psi_1 v_1 \\ -\lambda_x r_1 - \cos\psi_1 v_1 + \cos\psi_1 u_1 \\ -w_1 \\ -r_1 \end{bmatrix}, \quad \boldsymbol{\Delta}(t) = \begin{bmatrix} \Lambda_x \\ \Lambda_y \\ \Lambda_z \\ \Lambda_\psi \end{bmatrix} \\ &\mathbf{u}(t-\tau) \triangleq \begin{bmatrix} u_x|_{t-\tau} \\ u_y|_{t-\tau} \\ u_z|_{t-\tau} \\ u_\psi|_{t-\tau} \end{bmatrix} \triangleq \begin{bmatrix} \cos\psi_1 u_2 + \sin\psi_1 v_2|_{t-\tau} \\ \cos\psi_1 v_2 - \sin\psi_1 u_2|_{t-\tau} \\ w_2|_{t-\tau} \\ r_2|_{t-\tau} \end{bmatrix} \end{aligned} \tag{7}$$

As the communication delay exists, the feedback states are not reliable, and cannot be used to deal with $f(\boldsymbol{\lambda})$. However, $f(\boldsymbol{\lambda})$ and $\boldsymbol{\Delta}(t)$ can be treated as combined disturbance and observed by extended state observer (ESO).

For the time-delay, taking virtual control $\mathbf{U}(t)=\mathbf{u}(t-\tau)$ into (7), the system can be converted into a non-delay system. In the meantime, the ESO are specially designed for the

formation system to reject the combined disturbance. Taking the ESO design of x channel for example

$$\begin{cases} e_{1x} = \sigma_1 - \lambda_x \\ \sigma_1 = \sigma_1 + h(-\beta_{1x} e_{1x} + U_x + \sigma_2) \\ \sigma_2 = \sigma_2 - h\beta_{2x} fal(e_{1x}, \alpha_{ob}, \delta_{ob}) \\ fal(e_{1x}, \alpha, \delta) = \begin{cases} |e|^{\alpha_{ob}} \operatorname{sgn}(e_{1x}) & |e_{1x}| > \delta_{ob} \\ \dfrac{e_{1x}}{\delta^{1-\alpha_{ob}}} & |e_{1x}| \le \delta_{ob} \end{cases} \end{cases} \tag{8}$$

where h is the sample period. The ESO guarantees that σ_1 tracks λ_x and σ_2 tracks $f(\boldsymbol{\lambda})_x + \Lambda_x$. Denoting $\boldsymbol{\lambda}_{\mathbf{d}} = (\lambda_{xd}, \lambda_{yd}, \lambda_{zd}, \lambda_{\psi d})^T$, the virtual control $U_x(t)$ is

$$\begin{aligned} e_x &= \lambda_{xd} - \sigma_1 \\ U_x(t) &= k_x fal(e_x, \alpha_x, \delta_x) - \sigma_2 \end{aligned} \tag{9}$$

For the time-delay exists, $U_x(t)$ cannot catch up with the formation system. So the real control u_x can be predicted based on U_x. The predictive law can be denoted as

$$\begin{aligned} &u_x(s)e^{-\tau s} = U_x(s),\ e^{\tau s} \approx 1 + \tau s \\ &u_x(t) = U_x(t) + \tau \dot{U}_x(t) \end{aligned} \tag{10}$$

The tracking differentiator (TD) is designed to arrange transient processes for $U_x(t), \dot{U}_x(t)$.

$$\begin{aligned} x_1(k+1) &= x_1(k) + h x_2(k) \\ x_2(k+1) &= x_2(k) + h fst(x_1(k) - U_x(t), x_2(k), r, h_0) \end{aligned} \tag{11}$$

in which the definition of function fst can be found in [11], $x_1(k)$ and $x_2(k)$ are states of arranged process, x_1 tracks $U_x(t)$ and x_2 tracks its derivate $\dot{U}_x(t)$. h is the sample period, r and h_0 are called "speed factor" and "filter factor" respectively, which decide the tracking performance. Then the discrete form of u_x can be rewritten as

$$u_x(k) = x_1(k) + \tau x_2(k) \tag{12}$$

The analysis of u_y, u_z, u_ψ in other three channels is just the same as the design of u_x in (8-12). $(u_x, u_y, u_z, u_\psi)^T$ is the control vector of the formation system (7). The reference trajectory $(u_2, v_2, w_2, r_2)^T$ of the follower can be converted from u_x, u_y, u_z, u_ψ as (7). Assume that ψ_1 is the slowly varying signal and the time-delay makes few differences in ψ_1. The reference trajectory of the follower can be given as

$$\begin{cases} u_2 = u_x \cos\psi_1 - u_y \sin\psi_1 \\ v_2 = u_x \sin\psi_1 + u_y \cos\psi_1 \\ w_2 = u_z \\ r_2 = u_\psi \end{cases} \tag{13}$$

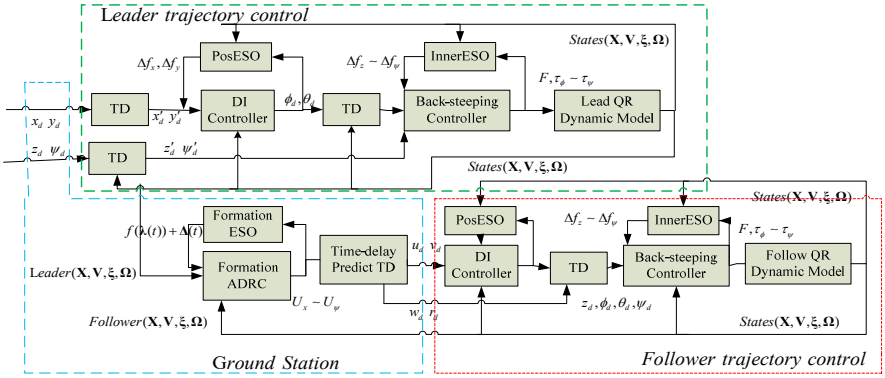

Figure 1. Integrated cooperative control scheme for the multiple quadrotors

B. Stability Analysis of the Formation Control System

The observed states are denoted as $\hat{\boldsymbol{\lambda}} = \begin{bmatrix} \hat{\lambda}_x & \hat{\lambda}_y & \hat{\lambda}_z & \hat{\lambda}_\psi \end{bmatrix}^T$, the observed disturbances are $\mathbf{d} = \begin{bmatrix} d_x & d_y & d_z & d_\psi \end{bmatrix}^T$, and the observed errors can be formulated as

$$\begin{aligned} \mathbf{z}_1 &= \hat{\boldsymbol{\lambda}} - \boldsymbol{\lambda} = \begin{bmatrix} z_{1x} & z_{1y} & z_{1z} & z_{1\psi} \end{bmatrix}^T \\ \mathbf{z}_2 &= \mathbf{d} - (f(\boldsymbol{\lambda}(t)) + \boldsymbol{\Delta}(t)) = \begin{bmatrix} z_{2x} & z_{2y} & z_{2z} & z_{2\psi} \end{bmatrix}^T \end{aligned} \tag{14}$$

A Lyapunov function is defined as

$$\begin{aligned} V = {} & \beta_{1x} \int_0^{z_{1x}} fal(z_{1x}, \alpha_{ob}, \delta_{ob}) dz_{1x} + \beta_{1y} \int_0^{z_{1y}} fal(z_{1y}, \alpha_{ob}, \delta_{ob}) dz_{1y} \\ & + \beta_{1z} \int_0^{z_{1z}} fal(z_{1z}, \alpha_{ob}, \delta_{ob}) dz_{1z} + \beta_{1\psi} \int_0^{z_{1\psi}} fal(z_{1\psi}, \alpha_{ob}, \delta_{ob}) dz_{1\psi} + \frac{1}{2} \mathbf{z}_2^{\mathrm{T}} \mathbf{z}_2 \end{aligned} \tag{15}$$

For $\int_0^x fal(x, \alpha_{ob}, \delta_{ob}) dx \ge 0, V \ge 0, i = x, y, z, \psi$

$$\begin{aligned} \dot{V} &= \beta_{2x} fal(z_{1x}, \alpha_{ob}, \delta_{ob}) \dot{z}_{1x} + \beta_{2y} fal(z_{1y}, \alpha_{ob}, \delta_{ob}) \dot{z}_{1y} \\ &+ \beta_{2z} fal(z_{1z}, \alpha_{ob}, \delta_{ob}) \dot{z}_{1z} + \beta_{2\psi} fal(z_{1\psi}, \alpha_{ob}, \delta_{ob}) \dot{z}_{1\psi} + \mathbf{z}_2^{\mathrm{T}} \dot{\mathbf{z}}_2 \\ &= \sum \beta_{2i} fal(z_{1i}, \alpha_{ob}, \delta_{ob})(-\beta_{1i} z_{1i} + z_{2i}) + \mathbf{z}_2^{\mathrm{T}} \dot{\mathbf{d}} \\ &= \sum (\beta_{2i} fal(z_{1i}, \alpha_{ob}, \delta_{ob})(-\beta_{1i} z_{1i} + z_{2i}) - z_{2i} \beta_{2i} fal(z_{1i}, \alpha_{ob}, \delta_{ob})) \\ &= -\sum \beta_{1i} \beta_{2i} z_{1i} fal(z_{1i}, \alpha_{ob}, \delta_{ob}) \end{aligned} \tag{16}$$

As $fal(z_{1i}, \alpha_{ob}, \delta_{ob})$ is the odd function, which satisfies

$$z_{i1} fal(z_{i1}, \alpha, \delta) \ge 0 \tag{17}$$

$\dot{V} = -\sum \beta_{1i} \beta_{2i} z_{1i} fal(z_{1i}, \alpha, \delta) \le 0$ when $\beta_{1i}, \beta_{2i} > 0$. As a result, the ESO observer errors for the system (7) are guaranteed asymptotically stable.

Then each channel of the system (7) can be rewritten as

$$\begin{aligned}\dot{\lambda}_i &= f(\lambda_i)+\Delta_i+U_i \\ &= (f(\lambda_i)+\Delta_i-d_i)+k_i fal(\lambda_{id}-\hat{\lambda}_i,\alpha,\delta)\end{aligned} \tag{18}$$

As the stability of the ESO is proved, the errors are denoted as $\mathbf{e}=\boldsymbol{\lambda}_\mathbf{d}-\boldsymbol{\lambda}=\begin{bmatrix}e_x & e_y & e_z & e_\psi\end{bmatrix}^T$ and then the system (18) can be rewritten as

$$\dot{\lambda}_i = k_i fal(e_i,\alpha,\delta) \tag{19}$$

Select the Lyapunov function $V=\frac{1}{2}\mathbf{e}^\mathbf{T}\mathbf{e}$, $V\geq 0$, when $k_i>0$

$$\begin{aligned}\dot{V} &= \mathbf{e}^\mathbf{T}\dot{\mathbf{e}} = \sum e_i\dot{e}_i = -\sum e_i\dot{\lambda}_i \\ &= -\sum k_i e_i fal(e_i,\alpha,\delta)\leq 0\end{aligned} \tag{20}$$

So the stability of formation control law is guaranteed.

IV. Design of The Trajectory Tracking Controller

The dynamic model of the quadrotor is under-actuated. To cope with this, the quadrotor system is decoupled into two fully actuated control loops with "time-scale separation principle". The outer loop is the position loop, which is affine form and can be controlled by dynamic inversion (DI). The position loop provides desired roll and pitch angles to the inner loop. For the inner loop, the control law is designed based on back-stepping control law and the Lyapunov stability analysis. What's more, the ESO are designed for both the outer loop and the inner loop, which estimate the unmodeled dynamics and the outer disturbances, and realize the robust trajectory tracking control.

A. DI Control Laws of the Outer Loop

The dynamic model of position loop can be written from (5). Denoting $\boldsymbol{\chi}=\begin{bmatrix}u & v\end{bmatrix}^T$, $\mathbf{\Delta f}=\begin{bmatrix}\Delta f_x & \Delta f_y\end{bmatrix}^T$, F as the feedback thrust, the virtual control $\mathbf{U}=\begin{bmatrix}U_1 & U_2\end{bmatrix}^T$ can be introduced as

$$\begin{aligned}U_1 &= F\sin\phi/m \\ U_2 &= F\sin\theta\cos\phi/m\end{aligned} \tag{21}$$

The position loop system satisfies the affine form

$$\begin{cases}\dot{x}=u \\ \dot{y}=v \\ \dot{\boldsymbol{\chi}}=G_1\mathbf{U}+\mathbf{\Delta f}\end{cases} \tag{22}$$

$$\begin{bmatrix}\dot{u}\\ \dot{v}\end{bmatrix}=\begin{bmatrix}\sin\psi & \cos\psi\\ -\cos\psi & \sin\psi\end{bmatrix}\begin{bmatrix}U_1\\ U_2\end{bmatrix}+\begin{bmatrix}\Delta f_x\\ \Delta f_y\end{bmatrix}$$

The position ESO is designed to estimate disturbance $\mathbf{\Delta f}$, taking the design of x channel ESO for example

$$\begin{cases}e=z_{x1}-u \\ z_{x1}=z_{x1}-\beta_{01}e+h(U_1\sin\psi+U_2\cos\psi+z_{x2}) \\ z_{x2}=z_{x2}-h\beta_{02}fal(e,\alpha,\delta)\end{cases} \tag{23}$$

in which the definition of h and $fal(e,\alpha,\delta)$ is the same as (8). The ESO guarantees that z_{x1} tracks u and z_{x2} tracks Δf_x. Similarly, the ESO for y channel is also designed to guarantee that z_{y2} tracks Δf_y. Denoting $\mathbf{v}=\begin{bmatrix}v_x & v_y\end{bmatrix}^T$, the observed disturbance vector as $\mathbf{z_2}=\begin{bmatrix}z_{x2} & z_{y2}\end{bmatrix}^T$, the desired position $\begin{bmatrix}x_d & y_d\end{bmatrix}^T$, and then the dynamic inversion (DI) control law can be designed as

$$\begin{aligned}&\mathbf{U}=G_1^{-1}(\mathbf{v}-\mathbf{z_2}) \\ &v_x=\ddot{x}_d-k_{x1}(\dot{x}-\dot{x}_d)-k_{x2}(x-x_d) \\ &v_y=\ddot{y}_d-k_{y1}(\dot{y}-\dot{y}_d)-k_{y2}(y-y_d)\end{aligned} \tag{24}$$

The relative degree $r_x+r_y=4$, so no zero dynamic exists. $|G_1|\equiv 1$, so G_1^{-1} always exists. When $k_{x1},k_{x2},k_{y1},k_{y2}>0$, the error equations are Hurwitz and exponentially stable. The desired roll and pitch and angles can be given as

$$\phi_d=\arcsin(\frac{mU_1}{F}),\ \theta_d=\arcsin(\frac{mU_2}{\sqrt{F^2-(mU_1)^2}}) \tag{25}$$

B. Back-stepping Control Laws of the Inner Loop

When the inner loop state is denoted as $\mathbf{x_1}=\begin{bmatrix}z & \phi & \theta & \psi\end{bmatrix}^T$, the inner loop system can be described as

$$\begin{cases}\dot{\mathbf{x}}_1=\mathbf{x}_2 \\ \dot{\mathbf{x}}_2=f(\mathbf{x_1},\mathbf{x_2})+g(\mathbf{x_1},\mathbf{x_2})\mathbf{u}+\mathbf{\Delta d}\end{cases}$$

$$f(\mathbf{x_1},\mathbf{x_2})=\begin{bmatrix}-g\\ \frac{I_y-I_z}{I_x}qr\\ \frac{I_z-I_x}{I_y}pr\\ \frac{I_x-I_y}{I_z}pq\end{bmatrix},\ g(\mathbf{x_1},\mathbf{x_2})=\begin{bmatrix}\frac{m}{\cos\theta\cos\phi}\\ 1/I_x\\ 1/I_y\\ 1/I_z\end{bmatrix} \tag{26}$$

$$\mathbf{u}=\begin{bmatrix}F & \tau_\phi & \tau_\theta & \tau_\psi\end{bmatrix}^T,\mathbf{\Delta d}=\begin{bmatrix}\Delta f_z & \Delta f_\phi & \Delta f_\theta & \Delta f_\psi\end{bmatrix}^T$$

The inner loop system is the strict-feedback system. The ESO can be designed for the inner loop system to observe uncertainty $\mathbf{\Delta d}$ and eliminate it. Taking the design of z channel for example

$$\begin{cases}e_z=v_1-z \\ v_1=v_1+h(-\beta_1 e_z+v_2) \\ v_2=v_2+h(-\beta_2 fal(e_z,\alpha_1,\delta)+f(z)+g(z)u_z+v_3) \\ v_3=v_3-h\beta_3 fal(e_z,\alpha_2,\delta)\end{cases} \tag{27}$$

$$f(z)=-g,g(z)=\frac{m}{\cos\theta\cos\phi}$$

The ESO guarantees that v_3 tracks Δf_z. The ESOs for other channels can be designed just as (27). The observed disturbances can be written as $\boldsymbol{\sigma}_\mathbf{f}=\begin{bmatrix}\sigma_{fz} & \sigma_{f\phi} & \sigma_{f\theta} & \sigma_{f\psi}\end{bmatrix}^T$. The desired states are denoted as $\mathbf{x_{1d}}=\begin{bmatrix}z_d & \phi_d & \theta_d & \psi_d\end{bmatrix}^T$, $\mathbf{x_{2d}}=\begin{bmatrix}w_d & p_d & q_d & r_d\end{bmatrix}^T$. The error equations are

$$\mathbf{e}_1 = \mathbf{x}_1 - \mathbf{x}_{1d}, \mathbf{e}_2 = \mathbf{x}_2 - \mathbf{x}_{2d} \tag{28}$$

Step1: select the Lyapunov function $V_1 = \frac{1}{2}\mathbf{e}_1^T\mathbf{e}_1$, $V_1 \geq 0$

$$\begin{aligned} \dot{V}_1 &= \mathbf{e}_1^T\dot{\mathbf{e}}_1 = \mathbf{e}_1^T(\mathbf{x}_2 - \dot{\mathbf{x}}_{1d}) \\ \dot{V}_1 &= -k_1\mathbf{e}_1^T\mathbf{e}_1 \leq 0, when\ \mathbf{x}_2 = -k_1\mathbf{e}_1 + \dot{\mathbf{x}}_{1d}, k_1 > 0 \end{aligned} \tag{29}$$

Step2: select the Lyapunov function $V_2 = \frac{1}{2}(\mathbf{e}_1^T\mathbf{e}_1 + \mathbf{e}_2^T\mathbf{e}_2)$

$$\begin{aligned} V_2 &\geq 0, \mathbf{x}_{2d} = -k_1\mathbf{e}_1 + \dot{\mathbf{x}}_{1d} \\ \dot{V}_2 &= \mathbf{e}_1^T\dot{\mathbf{e}}_1 + \mathbf{e}_2^T\dot{\mathbf{e}}_2 \\ &= \mathbf{e}_1^T(\mathbf{e}_2 + \mathbf{x}_{2d} - \dot{\mathbf{x}}_{1d}) + \mathbf{e}_2^T(\dot{\mathbf{x}}_2 - \dot{\mathbf{x}}_{2d}) \\ &= \mathbf{e}_1^T\mathbf{e}_2 - k_1\mathbf{e}_1^T\mathbf{e}_1 + \mathbf{e}_2^T(f(\mathbf{x}_1,\mathbf{x}_2) + g(\mathbf{x}_1,\mathbf{x}_2)\mathbf{u} + \boldsymbol{\sigma}_f + k_1\dot{\mathbf{e}}_1 - \ddot{\mathbf{x}}_{1d}) \\ &= -k_1\mathbf{e}_1^T\mathbf{e}_1 + \mathbf{e}_2^T(f(\mathbf{x}_1,\mathbf{x}_2) + g(\mathbf{x}_1,\mathbf{x}_2)\mathbf{u} + \boldsymbol{\sigma}_f + \mathbf{e}_1 + k_1\dot{\mathbf{e}}_1 - \ddot{\mathbf{x}}_{1d}) \end{aligned} \tag{30}$$

Now the control vector $\mathbf{u}$ can be designed as

$$\begin{cases} u_z = \dfrac{m}{\cos\theta\cos\phi}(g - \sigma_{fz} + \ddot{z}_d - (z - z_d) - k_{z1}(\dot{z} - \dot{z}_d) - k_{z2}(w - w_d)) \\ u_\phi = I_x(\dfrac{I_z - I_y}{I_x}qr - \sigma_{f\phi} + \ddot{\phi}_d - (\phi - \phi_d) - k_{\phi1}(\dot{\phi} - \dot{\phi}_d) - k_{\phi2}(p - p_d)) \\ u_\theta = I_y(\dfrac{I_x - I_z}{I_y}pr - \sigma_{f\theta} + \ddot{\theta}_d - (\theta - \theta_d) - k_{\theta1}(\dot{\theta} - \dot{\theta}_d) - k_{\theta2}(q - q_d)) \\ u_\psi = I_z(\dfrac{I_y - I_x}{I_z}pq - \sigma_{f\psi} + \ddot{\theta}_d - (\psi - \psi_d) - k_{\psi1}(\dot{\psi} - \dot{\psi}_d) - k_{\psi2}(r - r_d)) \end{cases} \tag{31}$$

Taking (31) into (30), there is

$$\begin{aligned} \dot{V}_2 &= \mathbf{e}_1^T\mathbf{e}_2 - k_1\mathbf{e}_1^T\mathbf{e}_1 + \mathbf{e}_2^T(-\mathbf{e}_1 - \boldsymbol{\sigma}_f - k_2\mathbf{e}_2 + \dot{\mathbf{x}}_{2d} + \boldsymbol{\sigma}_f - \dot{\mathbf{x}}_{2d}) \\ &= -k_1\mathbf{e}_1^T\mathbf{e}_1 - k_2\mathbf{e}_2^T\mathbf{e}_2 \leq 0 \quad (k_1, k_2 > 0) \end{aligned} \tag{32}$$

For the back-stepping controller are designed based on the Lyapunov stability analysis, the error system of (26) is guaranteed asymptotically stable.

V. SIMULATIONS

Firstly, the simulation is designed to validate the performance of our trajectory tracking control for all the quadrotors themselves. The initial states are $\mathbf{X}=\mathbf{V}=\boldsymbol{\xi}=\boldsymbol{\Omega}=\mathbf{0}$. The reference state is $x_d = 3, y_d = 2, z_d = 2, \psi_d = 10\pi/180(rad)$. $\mathbf{\Delta f} = (0.1\text{sign}(\sin(t))), 0.1\text{sign}(\sin(t)), 0.2\sin(t))^T$ simulates the gusty wind disturbances. The contrast simulation is conducted under the two circumstances: 1) With ESO; 2) Without ESO. The model coefficients are given in Table 1.

TABLE 1. PARAMETERS OF THE TRAJECTORY TRACKING CONTROL

Quadrotor Model	*TD*	*DI Outer Loop*
$k_T = 5.5\times10^{-5}$	$r_\xi = 1,\ r_\Omega = 2$	$k_{x1} = k_{y1} = 3, k_{x2} = k_{y2} = 1.5$
$k_d = 1.1\times10^{-6}(m\cdot s^{-2})$	$r_{xy} = 0.1, r_z = 0.5$	$\alpha = 0.5, \delta = 0.5, h = 0.01$
$J_x = J_y = 8\times10^{-3}$	$h = 0.01, h_0 = 0.05$	$\beta_{01} = 100, \beta_{02} = 300$
$J_z = 1.4\times10^{-2}(kg\cdot m^2)$	***Back-stepping Inner Loop***	
$m = 1kg, l = 0.24m$	$k_{\phi1} = k_{\phi2} = 3, k_{\theta1} = k_{\theta2} = k_{z1} = k_{z2} = k_{\psi1} = k_{\psi2} = 10$	
	$\alpha_1 = \delta = 0.5, \alpha_2 = 0.25, h = 0.01$	
	β_1=200, β_2=600, β_3=2000	

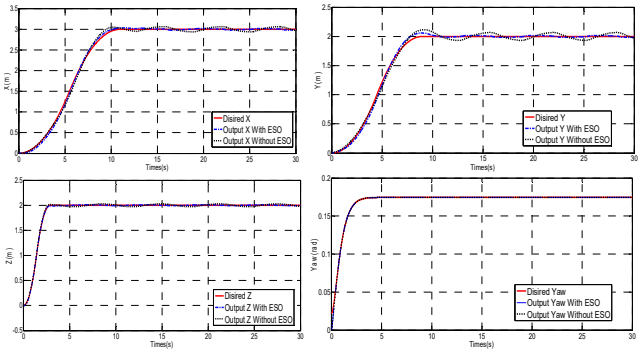

Figure 2. The trajectory tracking performances with ESO/without ESO

The Figure 2 shows the tracking performances under two circumstances in the four channels: x, y, z and ψ. It can be concluded that the controller with ESO gains better performance in trajectory tracking under disturbances than the controller without ESO. The two circumstances all performs well in the yaw channel for no disturbances influence the yaw.

Based on the reliable trajectory controller, the simulation is designed to show the performance of the formation control. Quadrotor 1 acts as the leader. Both Quadrotor 2 and 3 act as the followers. The formation control scheme is applied to the two leader-follower pairs (1, 2), (1, 3) synchronously, with time-delay τ_1, τ_2 existing in two pairs respectively. The time delay in pair (1, 2) is assumed greater than that of pair (1, 3) to test the predictive ADRC. Three different desired formations are designed in three time intervals [0, 15], [15, 30], [30, 50] to simulate the formation changes. The desired formation and the parameter of formation controller are given in Table 2.

TABLE 2. PARAMETERS OF THE FORMATION CONTROL

Formation Control	*Desired Formations in three time intervals*		
α_{ob}=0.65, δ_{ob}=0.005	0-15s	15-30s	30-50s
$\beta_{1x} = \beta_{1y} = \beta_{1z} = 200$	***Pair 1: Quadrotor (1 , 2)*** τ_1=0.15s		
$\beta_{2x} = \beta_{2y} = \beta_{2z} = 4$	$\lambda_x = -5, \lambda_y = -5$ $\lambda_z = 0, \lambda_\psi = 0$	$\lambda_x = 0, \lambda_y = -3$ $\lambda_z = 2, \lambda_\psi = 0$	$\lambda_x = 5, \lambda_y = -5$ $\lambda_z = 0, \lambda_\psi = 0$
$\alpha_x = \alpha_y = \alpha_z = 0.75$	***Pair 2: Quadrotors (1 ,3)*** τ_2=0.1s		
$\delta_x = \delta_y = \delta_z = 0.2$	$\lambda_x = 5, \lambda_y = -5$ $\lambda_z = 0, \lambda_\psi = 0$	$\lambda_x = 0, , \lambda_y = -6$ $\lambda_z = 4, \lambda_\psi = 0$	$\lambda_x = -5, \lambda_y = -5$ $\lambda_z = 0, \lambda_\psi = 0$
$\alpha_\psi = 0.85$ $\delta_\psi = 0.1$			

The Initial positions of the three quadrotors are $\mathbf{X}_1 = \mathbf{0}, \mathbf{X}_2 = (-3, 0, 0)^T$, $\mathbf{X}_3 = (3, 0, 0)^T$. The yaw angles are $\psi_1 = 10\pi/180, \psi_2 = \psi_2 = 0(rad)$. The desired trajectory for the leader is $\mathbf{X}_{1d} = (0.3t, 0.4t, 0.2t)^T$, $\psi_{1d} = 0$. The lead trajectory is time-varying, which makes it harder for the formation control. Furthermore, the disturbance $\mathbf{\Delta f}$ for each quadrotor is set the same as the former simulation. There are 2 formation changes in t=15s and t=30s.

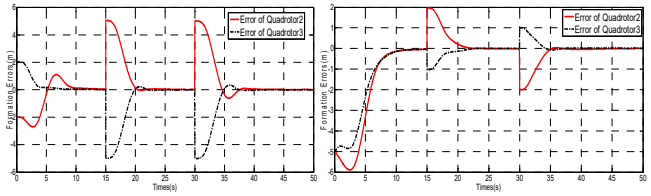

(a) X formation errors (b) Y formation errors

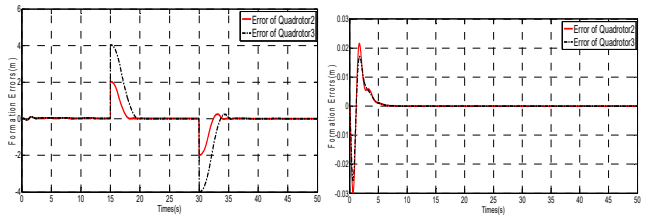

(c) Z formation errors (d) Yaw angle Formation errors

Figure 3. The formation errors during the three formation intervals

The formation errors jump high in t=15s and t=30s owing to the formation references switches. The errors return to zero rapidly faced with switches. The formation maintains well within each three time intervals for the errors are kept zero. The formations generate and reconstruct a little faster in pair (1, 3) than that of pair (1, 2) for the time delay τ_1=0.15s is greater than τ_2=0.1s **.** However, the influence of time delay is attenuated by the predictive ADRC. The formation errors are both converge to zero rapidly, thus constructing the three-quadrotor desired formations rapidly and precisely.

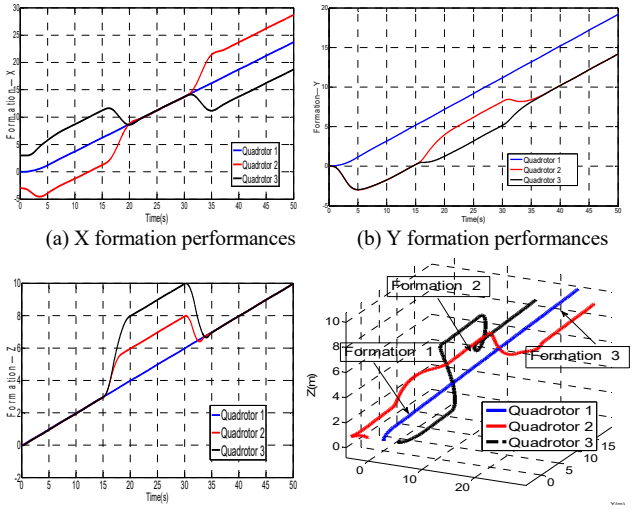

(a) X formation performances (b) Y formation performances

(c) Z formation performances (d) 3D performances

Figure 4. The performances of the formation control

Figure 4 shows the performances of the three-quadrotor formation control in x, y, z channels and in the 3D view. In the first time interval [0, 15s], the Formation 1 is generated rapidly, with Quadrotor 2 in the left side, Quadrotor 3 in the right side of Quadrotor 1.When t=15s, the first formation takes place. The Quadrotor 2, 3 climb just above the Quadrotor 1 and reconstruct the Formation 2. The second formation change in t=30s is similar to the first one. The 3D performance shows that the desired formation are generated rapidly in the Formation 1.The three-quadrotor formation switches smoothly and maintains stably during the whole simulation.

VI. Conclusions

In this paper, an integrated cooperative control scheme of multiple quadrotors is proposed. Firstly, the formation model is established based on the classical "leader-follower" theory. What makes it different is that our formation model takes the trajectory tracking errors, the state measurement errors, and the communication time delays into account. Secondly, referring to the adaptive disturbance rejection control (ADRC), the extended state observer (ESO) and nonlinear control law is designed to eliminate the disturbances and improve the robustness of the formation controller. Furthermore, the tracking differentiators (TDs) play an important role in our scheme, which arrange transient process for states and are utilized for the improved ADRC to cope with time delay. The references for the followers are generated by the formation control. Thirdly, the double-loop control law, which is composed of DI control law in the position loop, back-stepping control law in the inner loop and the ESO for disturbance rejection, realizes the robust trajectory tracking control. The stabilities of the formation control and the trajectory tracking control are analyzed by the Lyapunov method. Finally, the simulations show performances of the cooperative control. The precise formation maintenances and smooth formation switches also validate the effectiveness of our integrated cooperative control scheme.

References

[1] R. O. Saber, "Flocking for Multi-Agent Dynamic Systems: Algorithms and Theory," *IEEE Trans. Automatic Control,* vol. 51, no. 3, pp. 401–420, 2006.

[2] J. A. Guerrero, P. Castillo, S. R. Lozano, "Mini Rotorcraft Flight Formation Control Using Bounded Inputs," *Intell Robot Syst. J,* vol. 65, no. 14, pp. 175–186, 2012

[3] M. Turpin, N. Michael, V. Kumar, "Trajectory Design Control for Aggressive Formation Flight with Quadrotors," *Autonomous Robots. J,* vol. 33, no. 1-2, pp. 143–156, 2012

[4] W. B. Dunbar, R. M. Murray, "Model Predictive Control of Coordinated Multi-vehicle Formations," in 2003 *Proc. Conf. Control and Decision,* pp. 4631–4636, January, 2003

[5] J. P. Desai, J. P. Ostrowski, "Modeling and control of formations of non-holonomic mobile robots," *IEEE Trans. Robotics and Automation,* vol. 17, no. 6, pp. 905–908, 2001.

[6] N. E. Leonard, E. Fiorelli, "Virtual Leaders, Artificial Potentials and Coordinated Control of Groups," in 2001 *Proc. Conf. Control and Decision,* pp.2968–2973, 2003

[7] T. Balch, R. C. Arkin, "Behavior-based Formation Control for multi-robot teams," *IEEE Trans. Robotics and Automation,* vol. 14, no. 6, pp. 926–939, 1999

[8] X. Chen, A. Serrani, "ISS-Based Robust Leader/Follower Trailing Control," *LNCIS 336 Group Coordination and Cooperative Control,* Germany: Springer-Verlag, 2006

[9] J. A. Guerrero, I. Fantoni, S. Salazar, R. Lozano, "Flight Formation of Multiple Mini Rotorcraft via Coordination Control," in *Intel Conf. Robotics and Automation,* pp. 620–625, 2010

[10] J. Han, "From PID to Active Disturbance Rejection Control," *IEEE Trans. Industrial Electronics,* vol. 56, no. 3, pp. 900–906, 2009

[11] S. Zhao, Z. Gao, "Modified active disturbances rejection control for time-delay systems," *ISA Transactions.* vol. 53, no. 4, pp. 882–888, 2014

[12] A. Basri, A. R. Husain, K. A. Danapalasingam, "Enhanced Backstepping Controller Design with Application to Autonomous Quadrotor Unmanned Aerial Vehicle," *Intell Robot Syst. J,* vol. 79, no. 2, pp. 295–321, 2014

[13] S. Bouabdallah, R. Siegwart, "Backstepping and Sliding-mode Techniques Applied to an Indoor Micro Quadrotor," in 2005 *Intel Conf. Robotics and Automation.* pp. 2247-2252, 2005

[14] H. Du, Z. Pu, J. Yi, H. Qian, "Advanced Quadrotor Based on Incremental Nonlinear Dynamic Inversion and Integral Extended State Observer," *Intel Conf. Guidance, Navigation and Control,* pp.1881-1886, Nanjing, 2016